Oscillatory Activity in Electrosensory Neurons Increases with the Spatial Correlation of the Stochastic Input Stimulus

Brent Doiron,[1,2] Benjamin Lindner,[1] André Longtin,[1] Leonard Maler,[2] and Joseph Bastian[3]
[1]*Physics Department, University of Ottawa, 150 Louis Pasteur, Ottawa, Ontario, Canada K1N 6N5*
[2]*Department of Cellular and Molecular Medicine, University of Ottawa, 451 Smyth Road, Ottawa, Ontario, Canada K1H 8M5*
[3]*Department of Zoology, University of Oklahoma, Norman, Oklahoma 73019, USA*
(Received 6 August 2003; published 20 July 2004)

We present results from a novel experimental paradigm to investigate the influence of spatial correlations of stimuli on electrosensory neural network dynamics. Further, a new theoretical analysis for the dynamics of a model network of stochastic leaky integrate-and-fire neurons with delayed feedback is proposed. Experiment and theory for this system both establish that spatial correlations induce a network oscillation, the strength of which is proportional to the degree of stimulus correlation at constant total stimulus power.

DOI: 10.1103/PhysRevLett.93.048101 PACS numbers: 87.18.Hf, 02.30.Ks, 02.50.Ey, 87.19.Bb

The nontrivial effects of noise on the dynamics of physical, chemical, and biological systems are beginning to be uncovered [1]. In particular, stochastic forcing can sometimes produce qualitative dynamics that are absent in the deterministic system. Neural networks [2–5] are ideal for the study of stochastic dynamics in spatially extended systems, since noise constitutes a significant component of neural activity. However, while specific dynamics have been linked to combinations of network architecture and stochastic forcing, direct functional interpretation of the noise-induced dynamics are often lacking. A common feature of neural network architecture is that higher-order stages of processing influence lower-order stages through delayed feedback projections [6–8]. Much theoretical work has focused on the dynamics that such a recurrent connectivity produces, both with [4,9,10] and without [11] explicit axonal delays. Nevertheless, the functional role that delayed feedback plays in biological neural networks is poorly understood. Thus, the combination of stochastic forcing and delayed network interactions is a timely yet relatively unexplored area of study.

In a recent study, we showed how diffuse delayed inhibitory feedback caused oscillatory spike trains from electrosensory neurons in response to stochastic communicationlike, but not preylike, stimuli [12]. It was hypothesized that the key distinguishing feature between these two inputs was that communication stimuli correlate the activity of many neurons while prey stimuli do not. However, in [12], we were unable to separate this correlation from the fact that communication stimuli have a greater degree of spatial power since they cover large portions of the sensory field [13]. This is in contrast to prey which are spatially compact stimuli. In this Letter, we show through a combination of novel experimental and theoretical analyses that it is indeed the spatial correlation in stimuli and not the total spatial power that is essential for oscillatory network spiking.

Experiments.—The weakly electric fish *Apteronotus leptorhynchus* has an electric organ that discharges a quasisinusoidal electric field (between 600 and 1000 Hz) surrounding its body [14]. Nearby objects or communicating fish distort this field so that an effective electric image is projected on the surface of the skin. These distortions are amplitude modulations (AMs) of the carrier field and are recorded by arrays of electroreceptors that line the surface of the skin. The electroreceptor afferents project to pyramidal cells of the electrosensory lateral line lobe (ELL) which process input and then project to higher brain centers [8]. These centers then output back to the ELL pyramidal cell layer producing an effective closed loop architecture for peripheral electrosensory processing.

To explore the effects of stochastic stimuli with variable spatial correlation, an array of four dipoles was constructed and placed near the surface of the skin [Fig. 1(a)]. The jth dipole in the array ($j = 1, \ldots, 4$) emitted a random AM, $I_j(t)$, consisting of two distinct stochastic processes, one intrinsic to the dipole, $\xi_i(t)$, and one common to all dipoles, $\xi_G(t)$. Specifically, we write

$$I_j(t) = \sigma[\sqrt{1-c}\,\xi_j(t) + \sqrt{c}\,\xi_G(t)], \tag{1}$$

where σ is the total intensity of the applied stimulus I_j measured in units of $\mathrm{V\,cm^{-1}}$ (σ is kept constant for our study). Both $\xi_i(t)$ and $\xi_G(t)$ are zero mean and Gaussian with a frequency content that was uniformly distributed between 0–60 Hz (eighth order Butterworth filter). We set $\langle \xi_j(t)\xi_G(t)\rangle = 0$ and $\langle \xi_j(t)\xi_k(t)\rangle = \delta_{jk}$. This implies that $\langle I_j(t)I_k(t)\rangle/\langle I_j(t)^2\rangle = c$, where c is the normalized covariance between any two dipoles in the array. Stimuli are spatially uncorrelated for $c = 0$, similar to that produced by a root mass or rocky substrate, while c near one mimics a communication signal. We remark that the total spatial power of the input, $4\sigma^2$, is independent of c.

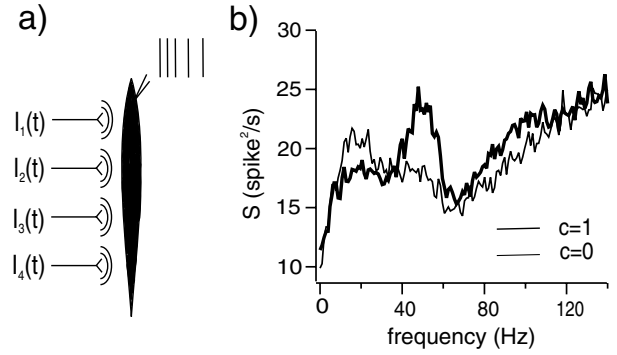

FIG. 1. Spatial correlation of stimuli determines oscillatory activity in electrosensory neurons. (a) Schematic of experimental stimulation. Single unit activity was recorded from ELL pyramidal cells while one side of the fish was stimulated with an array of four dipoles. Each dipole had a tip spacing of approximately 1.2 cm and the centers of adjacent dipoles were separated by 2.2 cm. Each dipole was 1.5 cm from the skin surface and stimulated roughly 2 cm^2 of the skin for typical stimulus contrasts (250 $\mu V\,cm^{-1}$). This ensured that there was limited overlap of the distinct dipole's electric images on the skin. (b) Spike train power spectra, S, when the spatial correlation between the dipoles, c, was set to 0 (light curve) and one (dark curve).

Single unit *in vivo* extracellular recordings from ELL pyramidal cells were obtained for various c values; experimental techniques are as in [12]. Figure 1(b) shows the power spectrum of a spike train from a typical pyramidal cell ($n = 7$) to stimuli with spatial correlation $c = 0$ and $c = 1$.

A weak low-frequency oscillation is apparent when $c = 0$. This oscillation is reduced and replaced with a high-frequency oscillation when $c = 1$. To quantify this shift in power with c, we introduce the statistic $\Gamma_{f_1,f_2,c} = \int_{f_1}^{f_2} S(f)\,df$, where $S(f)$ depends on c. A shift in $S(f)$ between $c = 0$ and $c = 1$ gives a nonzero value in $\Delta\Gamma_{f_1,f_2} = \Gamma_{f_1,f_2,1} - \Gamma_{f_1,f_2,0}$. Over our data ensemble ($n = 7$), we have that for low frequencies $\Delta\Gamma_{2,22} = -55.8 \pm 20.7$ (spikes^2/s^2) and for high frequencies $\Delta\Gamma_{40,60} = 53.7 \pm 30.8$ (spikes^2/s^2). These statistics are both significantly different from zero ($p_{2,22} = 3.9 \times 10^{-4}$ and $p_{40,60} = 7.3 \times 10^{-3}$; pairwise t test). We note that the relative difference in spike rate for $c = 0$ and $c = 1$ was only $0.61 \pm 0.43\%$, indicating that the shift in power cannot be accounted for by changes in input intensity. In total, these results show that ELL pyramidal neurons redistribute spike train power from low to high frequencies as the spatial correlations of a global input increase.

Model.—Consider a nonautonomous homogeneous network of N leaky integrate-and-fire (LIF) neurons [10]. The dynamics of the membrane potential $V_j(t)$ of the jth neuron ($j = 1, \ldots, N$) evolves according to

$$\dot{V}_j = -V_j + \mu + \eta_j(t) + I_j(t) + \frac{g}{N}\sum_k^N K_{\tau_d} * x_k(t). \quad (2)$$

Time is measured in units of the membrane time constant (6 ms). The dynamics is complemented by the usual spike-and-reset rule: Whenever $V_j(t)$ reaches the threshold v_T, a spike is fired (the mth firing time of the jth neuron is denoted by $t_{j,m}$), and the neuron is in an absolute refractory state for time τ_R followed by a reset of V_j to the value v_R. The spike train of the jth neuron reads $x_j(t) = \sum \delta(t - t_{j,m})$ (the sum is taken over all spike times). In Eq. (2), the single neuron properties are described by $-V_j$, μ, and $\eta_j(t)$ standing for a leakage term, a constant base current, and an internal Gaussian white noise of intensity D, respectively. This intrinsic noise leads to spontaneous activity even in the absence of stimuli, as also observed in experiments [15]. Furthermore, we assume that the external stimulus $I(t)$ used in the experiments according to Eq. (1) is transduced by the afferents into an input current $I(t)$ of the same shape; instead of band limited noise, however, we use white noise in the model, for simplicity. The last term in Eq. (2) represents a mean-field-like feedback of the spike trains of all neurons which is convolved with a standard α function [10] and delayed by a time τ_d:

$$K_{\tau_d} * x(t) = \int_{\tau_d}^{\infty} d\tau\, x(t-\tau)\alpha^2\tau e^{-\alpha\tau}\Theta(\tau), \quad (3)$$

where $\Theta(t)$ is the Heaviside function [16]. The kernel K_{τ_d} is conceived as a composite process by which pyramidal cells first project their output to a "higher" brain center which integrates this input and then projects uniformly back to the original network via a common feedback pathway. This effective indirect interaction between cells via K_{τ_d} also involves a significant minimal delay term, τ_d, modeling both the integration time of the distant brain regions and finite axonal conduction velocity. The time scale of τ_d for the inhibitory pathway of interest is of the order of the membrane time constant (6 ms) [8,12]. The parameter α thus both represents a fast synaptic time scale and a distribution of delays. In this study, we confine $g < 0$ to model the inhibitory interactions of a specific feedback pathway previously shown to cause oscillatory network behavior [12]. Other known feedback pathways [8] are not treated (see [12] for biophysical justification). In order to allow for an analytical treatment, our model differs slightly from the one in Ref. [12]: Inhibition enters as an additive current term and the internal noise is white.

Theory.—In the steady state, we split the input currents into two parts: (i) base and leak currents, internal noise of strength D, and time-independent mean of the feedback $(-gr_0)[r_0 = \langle x(t)\rangle$ is the stationary firing rate of a single LIF neuron]; (ii) external signal and time-dependent part of the feedback. The first part constitutes a network of uncoupled white-noise driven LIF neurons with an effective base current $\mu' = \mu - gr_0(\mu')$ that has to be self-consistently determined from the well-known formula for the spike rate of a single LIF neuron $r_0(\mu') = [\tau_r + \sqrt{\pi}\int_{(\mu'-v_T)/\sqrt{D}}^{(\mu'-v_R)/\sqrt{D}} dx\, e^{x^2}\mathrm{erfc}(x)]^{-1}$ [erfc(x) is the complementary error function [16]]. With respect to the

time-dependent part of the feedback and the external input stimulus, we treat the system as a linear one characterized by the susceptibility $A(\omega)$ with respect to the input stimulus. Expressed by $\tilde{x}_{(0,)j} = \hat{F}(x_{(0,),j} - r_0)/\sqrt{T}$ ($\hat{F} = \int_0^T dt\, e^{i\omega t}$ denotes the Fourier transform; $x_j(t)$ and $x_{0,j}(t)$ are the spike train in the presence and absence of stimulus and feedback, respectively), this ansatz reads

$$\tilde{x}_j(\omega) = \tilde{x}_{0,j}(\omega) + A(\omega)\left[\tilde{I}_j(\omega) + \frac{g}{N}\tilde{K}_{\tau_d}(\omega)\sum_k \tilde{x}_k(\omega)\right], \tag{4}$$

where $\tilde{I}_j(\omega) = \hat{F}I_j(t)/\sqrt{T}$ and $\tilde{K}_{\tau_d}(\omega) = \hat{F}K_{\tau_d}(t)/\sqrt{T}$. Our choice of K_{τ_d} gives $\tilde{K}_{\tau_d}(\omega) = e^{i\omega\tau_d}/(1 - i\omega\alpha^{-1})^2$.

Equation (4) provides a system of equations relating $\langle\tilde{x}_j\tilde{x}_j^*\rangle$ (spike train power spectrum), $\langle\tilde{x}_j\tilde{x}_k^*\rangle$ ($j \neq k$; cross spectrum between distinct spike trains), and $\langle\tilde{x}_j\tilde{I}_j^*\rangle$ (cross spectrum between the stimulus and a spike train), where $*$ denotes complex conjugation. We further assume that $\langle\tilde{x}_{0,j}\tilde{x}_{0,k}^*\rangle = \langle\tilde{x}_{0,j}\tilde{I}_j^*\rangle = \langle\tilde{x}_j\tilde{\xi}_k^*\rangle = 0$ ($j \neq k$) and that $N \to \infty$ so as to neglect terms of order $1/N$ and higher. Finally, we replace the spectrum of the transmitted stimulus $S_0(\omega, D) + \sigma^2|A(\omega, D)|^2$, as it arises from pure linear response theory, by $S_0(\omega, Q)$, where $Q = D + \sigma^2/2$, representing the total noise intensity. Consequently, the susceptibility A is also evaluated at Q.

With these assumptions it can be shown [17] that the power spectrum of the spike train from a representative neuron, $S = \langle\tilde{x}_j\tilde{x}_j^*\rangle$ (with $T \to \infty$), is given by

$$S = S_0 + c\sigma^2|A|^2\frac{2\Re(g\tilde{K}_{\tau_d}A) - |g\tilde{K}_{\tau_d}A|^2}{|1 - g\tilde{K}_{\tau_d}A|^2}. \tag{5}$$

We let $S_0 = \langle\tilde{x}_0\tilde{x}_0^*\rangle$ and have dropped both the j notation and the ω dependence for S. Equation (5) shows that c simply sets the strength of the deviation of S from the uncoupled case (S_0). The precise form of the deviation is determined only by the internal (A) and feedback (K_{τ_d}) dynamics.

Equation (5) is applicable to a variety of neuron models; the special form of the LIF neuron allows for analytical expressions for both S_0 and A [18]:

$$S_0(\omega, Q) = r_0\frac{|\mathcal{D}_{i\omega}(\frac{\mu' - v_T}{\sqrt{Q}})|^2 - e^{2\Delta}|\mathcal{D}_{i\omega}(\frac{\mu' - v_R}{\sqrt{Q}})|^2}{|\mathcal{D}_{i\omega}(\frac{\mu' - v_T}{\sqrt{Q}}) - e^{\Delta}e^{i\omega\tau_R}\mathcal{D}_{i\omega}(\frac{\mu' - v_R}{\sqrt{Q}})|^2},$$

$$A(\omega, Q) = \frac{r_0 i\omega/\sqrt{Q}}{i\omega - 1}\frac{\mathcal{D}_{i\omega-1}(\frac{\mu' - v_T}{\sqrt{Q}}) - e^{\Delta}\mathcal{D}_{i\omega-1}(\frac{\mu' - v_R}{\sqrt{Q}})}{\mathcal{D}_{i\omega}(\frac{\mu' - v_T}{\sqrt{Q}}) - e^{\Delta}e^{i\omega\tau_R}\mathcal{D}_{i\omega}(\frac{\mu' - v_R}{\sqrt{Q}})},$$

where $\Delta = [v_R^2 - v_T^2 + 2\mu(v_T - v_R)]/4Q$ and $\mathcal{D}_a(z)$ denotes the parabolic cylinder function [16].

In Fig. 2(a), we show S computed via both simulations of the network model (2) and the theory as given by (5) when $c = 0$ and $c = 1$. The simulation and theory results match quite well for the chosen parameters. As c is increased, we see qualitative agreement with the experiments in several respects. For $c = 1$, the deviation term in (5) introduces a 50 Hz oscillation and a suppression of power at low frequencies, as compared to the $c = 0$ case. However, we note that the experimental results also contain a low-frequency oscillation when $c = 0$; this is not reproduced by either the simulations or the theory. The origins of this low-frequency oscillation are currently not known; however, our mathematical model of the ELL does not include other known feed forward and feedback pathways [8]. Figure 2(b) shows spike time raster plots from the simulations of Fig. 2(a). They show that for $c = 0$ there is relatively asynchronous behavior, whereas for $c = 1$ a degree of network synchrony is apparent. However, computing the average correlation coefficient between any two cells shows only an increase from approximately 10^{-4} to 0.065. The results of Fig. 2 were not sensitive to model parameters; the model presented in [12] shows similar behavior as does the present model for a range of μ values spanning both the sub- and suprathreshold ($\mu < v_T$ and $\mu > v_T$). Network oscillations emerging from relatively asynchronous sparsely connected stochastic delayed networks have been reported for a similar system [4], however, spatial correlation of the input was not considered; also in contrast, our network is not sparse. The effects of spatial correlation have been studied numerically in locally and electrically coupled networks of FitzHugh-Nagumo neurons [3] to be compared to the globally and inhibitory coupled network studied here. In [3], it was observed that regularized activity occurred for low input spatial correlations, in contrast to the results presented here.

A consequence of a linear response treatment of network (2) is that the shift in power is linear in c. To show

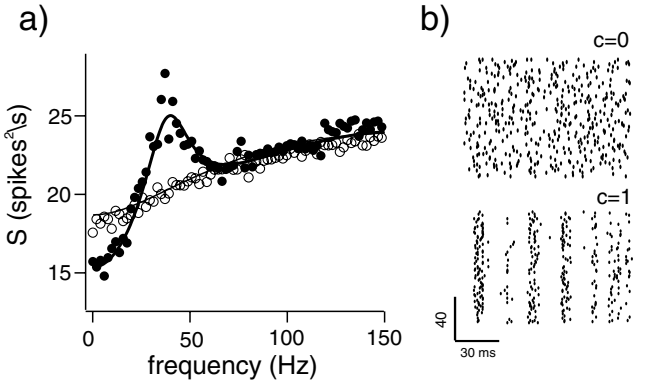

FIG. 2. Network model simulations and theoretical results for spatial correlation $c = 0$ and $c = 1$. (a) Spike train power spectra S for the network model given by (2) ($c = 0$, open circles; $c = 1$, closed circles) and the theoretical result (5) ($c = 0$, thin line; $c = 1$, thick line). (b) Network raster plots for the simulations shown in (a). The top plot is for $c = 0$ and the bottom plot is for $c = 1$. The parameters for both the simulations and theory were $v_R = 0$, $v_T = 1$, $\tau_R = 0.1$, $\mu = 0.5$, $g = -1.2$, $\alpha = 3$, $\tau_d = 1$, $D = 0.08$, $\sigma^2 = 0.16$, and $\mu' = 0.3286$. All simulations were integrated via a Euler integration scheme with a time step of 10^{-3}. The plots were rescaled so that the membrane time constant was 6 ms; note that $\omega = 2\pi f$.

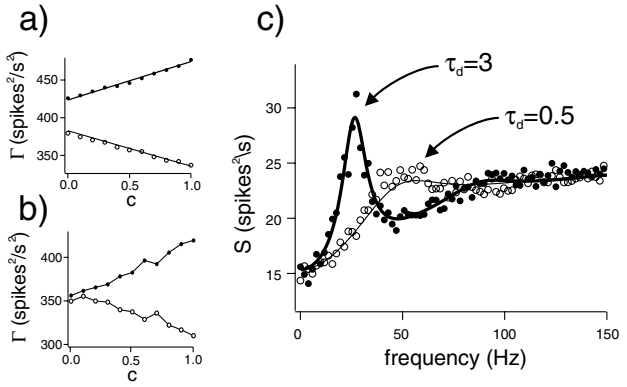

FIG. 3. Oscillation dependence on stimulus correlation and axonal delay. (a) $\Gamma_{f_1,f_2,c}$ plotted as a function of c for both $[f_1, f_2] = [2, 22]$ Hz (theory, thin line; simulations, open circles) and $[f_1, f_2] = [40, 60]$ Hz (theory, thick line; simulations, filled circles). Numerical integration of S computed from (5) was done with a fixed interval of $\Delta f = 0.1$ Hz, while integration of S determined from simulation of (2) used the fast-Fourier transform discretization step of $\Delta f = 0.5$ Hz. (b) Γ obtained from spike trains of ELL pyramidal cells for a range of c values. Data were obtained from same experiments as those for Fig. 1. (c) S shown for $\tau_d = 0.5$ (theory, thin curve; simulations, open circles) and $\tau_d = 3$ (theory, thick curve; simulations, filled circles). $c = 1$ for both curves. All other parameters are as given in Fig. 2.

this, we plot in Fig. 3(a) $\Gamma_{f_1,f_2,c}$ as a function of c for both low-frequency and high-frequency bands. There is good agreement between Γ obtained from the theory given by (5) and simulation of the network (2). The validity of our linear response ansatz for ELL pyramidal cells is supported experimentally when Γ is measured from ELL pyramidal neurons for a range of c values, shown in Fig. 3(b).

We finally study the dependence of the network oscillatory dynamics on the axonal delay τ_d. Figure 3(c) shows S for $\tau_d = 0.5$ and $\tau_d = 3$ (or in real time 3 and 18 ms, respectively). As expected, the frequency of oscillation decreases when τ_d increases, due to the $e^{i\omega\tau_d}$ term in K_{τ_d}. However, of interest is that the oscillation coherence (height of peak in S divided by peak half width) is significantly larger for larger τ_d. This is understood from the low pass nature of both the susceptibility A (specifically $|A|^2$) and the kernel K_{τ_d} (due to α). When we take $A \to 1$ and $\alpha \to \infty$ in Eq. (5), the coherence of the oscillation in S shows no dependence upon τ_d (results not shown).

Inhibitory feedback, with or without axonal delays, giving rise to network oscillations is a well studied phenomenon [4,9–11]. The effect of spatiotemporal stimuli on the dynamics of networks of noisy neurons, and, in particular, on the presence of oscillatory spiking, is poorly understood. Here we have shown using novel experimental and theoretical methods that the spatial correlation of the stimulus alone can induce such oscillations; this effect does not require an increase in the stimulus power integrated over space. Oscillatory network behavior in response to specific stimuli are now being catalogued in a variety of sensory systems [6,12,19]. Accounting for input-dependent dynamical phenomena, as shown here, will provide a deeper understanding of sensory brain function and, more generally, of nets of excitable elements.

We would like to thank J. Lewis, M. J. Chacron, J. Middleton, and A.-M. Oswald for discussions. This research was funded by NSERC (B. D., B. L., and A. L.), CIHR (L. M.), OPREA (B. L. and A. L.), and NIH (J. B.).

[1] J. García-Ojalvo and J. M. Sancho, *Noise in Spatially Extended Systems* (Springer-Verlag, New York, 1999); V. K. Vanag *et al.*, Nature (London) **406**, 389 (2000); A. Sanz-Anchelergues *et al.*, Phys. Rev. E **63**, 056124 (2001).

[2] P. Jung *et al.*, Phys. Rev. Lett. **74**, 2130 (1995); P. Tass, *Phase Resetting in Medicine and Biology* (Springer-Verlag, Berlin, 1999); A. B. Neiman *et al.*, Phys. Rev. Lett. **88**, 138103 (2002); M. P. Zorzano *et al.*, Physica D (Amsterdam) **179**, 105 (2003).

[3] C. Zhou *et al.*, Phys. Rev. Lett. **87**, 098101 (2001); H. Busch *et al.*, Phys. Rev. E **67**, 041105 (2003).

[4] N. Brunel *et al.*, Neural Comput. **11**, 1621 (1999).

[5] B.W. Knight, Neural Comput. **12**, 473 (2000).

[6] A. M. Sillito *et al.*, Nature (London) **369**, 479 (1994).

[7] E. Ahissar *et al.*, Cereb. Cortex **13**, 53 (2003); Le Masson *et al.*, Nature (London) **417**, 854 (2002).

[8] N. J. Berman *et al.*, J. Exp. Biol. **202**, 1243 (1999).

[9] M. Mackey *et al.*, J. Math Biol. **19**, 211 (1984); U. Ernst *et al.*, Phys. Rev. Lett. **74**, 1570 (1995); J. Foss *et al.*, Phys. Rev. Lett. **76**, 708 (1996).

[10] W. Gerstner and W. M. Kistler, *Spiking Neuron Models* (Cambridge Univerisity Press, New York, 2002).

[11] X.-J. Wang *et al.*, Neural Comput. **4**, 84 (1992); P. C. Bressloff *et al.*, Neural Comput. **12**, 91 (2000); D. J. Mar *et al.*, Proc. Natl. Acad. Sci. U.S.A. **96**, 10 450 (1999); J. Rinzel *et al.*, Science **279**, 1351 (1998); J. White *et al.*, J. Comput. Neurosci. **5**, 5 (1998).

[12] B. Doiron *et al.*, Nature (London) **421**, 539 (2003).

[13] G. K. H. Zupanc *et al.*, Can. J. Zool. **71**, 2301 (1993); W. Metzner, J. Exp. Biol. **202**, 1365 (1999).

[14] W. Heiligenberg, *Neural Nets in Electric Fish* (MIT Press, Cambridge, MA, 1991).

[15] J. Bastian *et al.*, J. Neurophysiol. **85**, 10 (2001).

[16] *Handbook of Mathematical Functions*, edited by M. Abramowitz and I. A. Stegun (Dover, New York, 1970).

[17] Eqs. (4) and (5) are due to Benjamin Lindner. Details will be given elsewhere.

[18] B. Lindner *et al.*, Phys. Rev. Lett. **86**, 2934 (2001); B. Lindner *et al.*, Phys. Rev. E **66**, 031916 (2002).

[19] M. Stopfer *et al.*, Nature (London) **390**, 70 (1997); H. Kashiwadani *et al.*, J. Neurophysiol. **82**, 1786 (1999); B. van Swinderen *et al.*, Nat. Neurosci. **6**, 579 (2003); K. MacLeod *et al.*, Science **274**, 976 (1996).